Supporting Materials

Intrinsic Stability Enhancement and Ionic Migration Reduction by Fluorinated Cations Incorporated in Hybrid Lead Halide Perovskites

Fedwa El-Mellouhi,[1]* Sergey N. Rashkeev,[1] Asma Marzouk,[1] Lara Kabalan,[1] Abdelhak Belaidi,[1] Belabbes Merzougui,[1] Nouar Tabet,[1,2] and Fahhad H. Alharbi[1,2]

[1]*Qatar Environment and Energy Research Institute (QEERI), Hamad Bin Khalifa University, Doha, Qatar*

[2]*College of Science and Engineering, Hamad Bin Khalifa University, Doha, Qatar*

*felmellouhi@hbku.edu.qa

1. Structural properties and on-site charges for MA and fluorinated cation

$[CH_3-NH_3]^+$

Atomic Charge (e)		Bonds lengths (Å)	
1N	-0.659	1N-2H	1.02007
2H	0.444	1N-3H	1.02003
3H	0.111	1N-4H	1.02003
4H	0.444	1N-5C	1.50223
5C	-0.388	5C-6H	1.08510
6H	0.239	5C-7H	1.08504
7H	0.239	5C-8H	1.08505
8H	0.239		

$[CFH_2-NH_3]^+$

Atomic Charge (e)		Bonds lengths (Å)	
1N	-0.695	1N-2H	1.02252
2H	0.452	1N-3H	1.02252
3H	0.452	1N-4H	1.020185
4H	0.452	1N-5C	1.50959
5C	0.243	5C-6H	1.08887
6H	0.200	5C-7H	1.08887
7H	0.200	5C-8F	1.33782
8F	-0.303		

$[CF_2H-NH_3]^+$

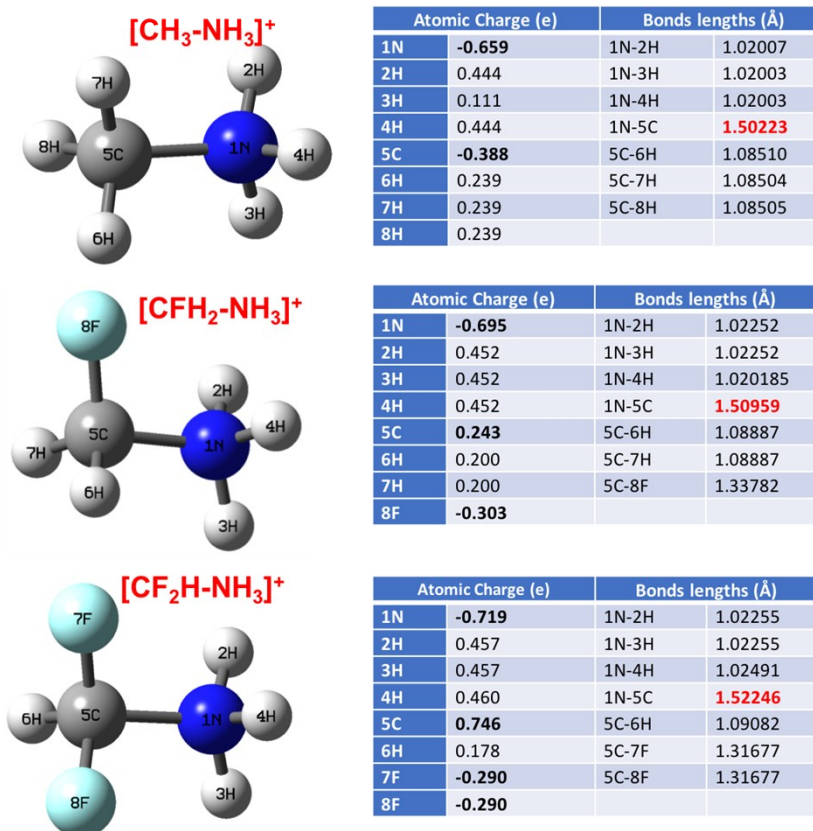| Atomic Charge (e)		Bonds lengths (Å)	
1N	-0.719	1N-2H	1.02255
2H	0.457	1N-3H	1.02255
3H	0.457	1N-4H	1.02491
4H	0.460	1N-5C	1.52246
5C	0.746	5C-6H	1.09082
6H	0.178	5C-7F	1.31677
7F	-0.290	5C-8F	1.31677
8F	-0.290		

Figure S1. Atomic charges at different atomic sites and interatomic distances in methylamine, mono-fluo methylamine and di-fluo-methylamine molecules.
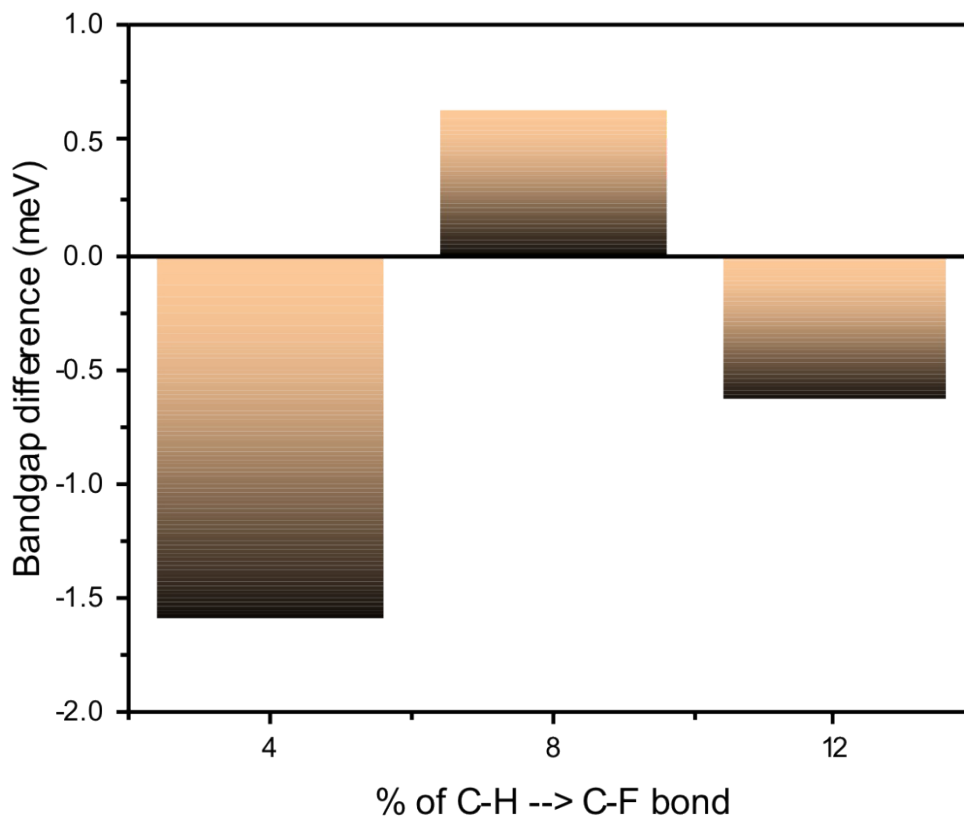

Figure S2. Bandgap variation (standard deviation in %) as a function of fluorination in $CH_3NH_3PbI_3$ perovskite. Fluorination contents of 4, 8, and 12% correspond to the substitution of one, two, and three hydrogen atoms in C-H bonds substituted by fluorine in tetragonal $CH_3NH_3PbI_3$ perovskite structural unitcell.

2. Noncovalent interactions (NCI) index calculations.

To characterize the strength of hydrogen bonds, we employed the recently developed noncovalent interactions (NCI) that enables real-space visualization of both attractive (van der Waals and hydrogen bonding) and repulsive interactions based on the electron density [1-3]. This approach allows description of the interplay between stabilizing and destabilizing contributions that determine the stable minima on hydrogen-bonding potential-energy surfaces.

It relies on two scalar fields to map local bonding properties: 1) the electron density (ρ) and 2) the so-called reduced density gradient (RDG, s) defined as

$$s(\text{RDG}) = \frac{1}{2(3\pi)^{1/3}} \frac{|\nabla\rho|}{\rho^{4/3}}. \tag{1}$$

Three principle interaction regions define the real space when combining the electron density and its gradient. The region of the non-interacting density tails is characterized by a high s and low \rho. However, a low s and high ρ define the covalent bonds region, where a low s and low ρ correspond to a non-covalent interaction. The non-covalent interactions are also classified into attractive or repulsive according to the sign of the second density eigenvalue (λ_2) of the electron-density Hessian (second derivative) matrix.

The calculations of the NCI index approach is not discussed in detail here. An important issue is that it allows differentiating van der Waals interactions and hydrogen bonds by densities at the corresponding bond critical point [1] Typically, characteristic densities of van der Waals interactions are much smaller than densities at which hydrogen bonds appear. At the same time, both van der Waals interactions and hydrogen bonds show negatives value λ_2 at the critical point, with a very low λ_2 (very near zero) for van der Waals interactions. A detailed analysis of the interaction type can be performed by plotting diagrams of s vs. sign(λ_2)ρ. When there is an overlap between atomic orbitals, a trough in the NCI diagram appears. The points forming this trough identify the interaction when they are mapped back to real space [1].

In practice, the computational procedure of constructing an NCI diagram requires a grid-based representation of the self-consistent electron density, which is obtained from quantum mechanical calculations. When the real-space region of interest is chosen, a regular grid is built to encompass it. At each grid point, ρ and s are numerically calculated and ρ is multiplied by the sign(λ_2).

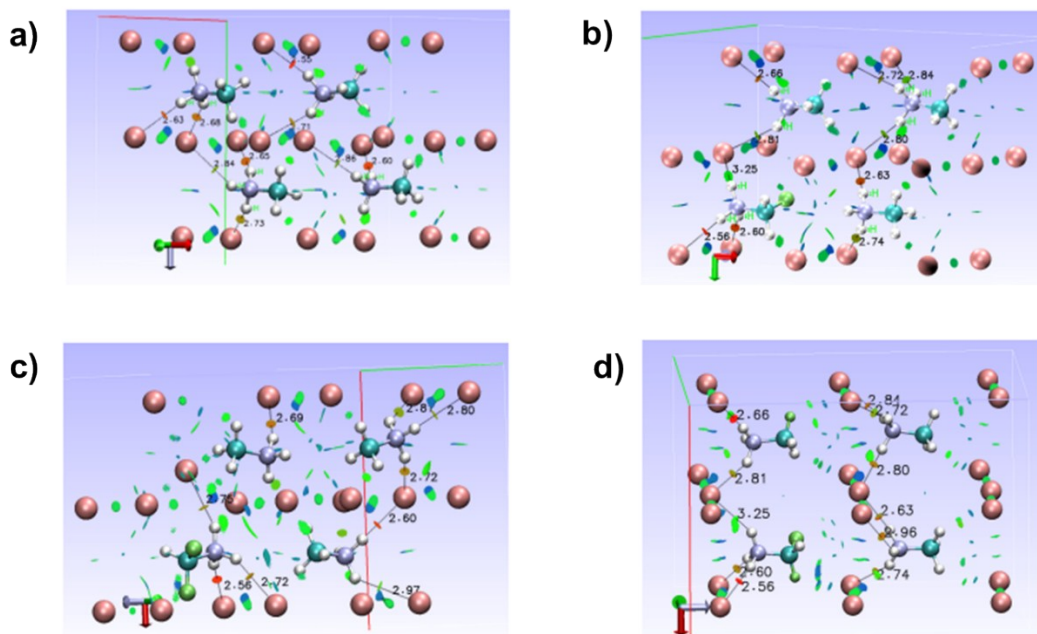**Figure S3.** NCI isosurfaces in real space for: a) tetragonal unitcell $CH_3NH_3PbI_3$, b), c), and d) same cell with one, two, or three $[CH_2F\text{-}NH_3]^+$ ions, respectively. Atoms C (cyan), N (blue), H (light pink), I (magenta), Br (brown), Cl (green), and F (purple). The isosurfaces are generated at s=0.3.

For visualization of the NCI regions we also plot RDG isosurfaces in real space, which allows interpretation of different feature in the NCI diagram as well as comparison of the strength of different NCI components (Figure S5).
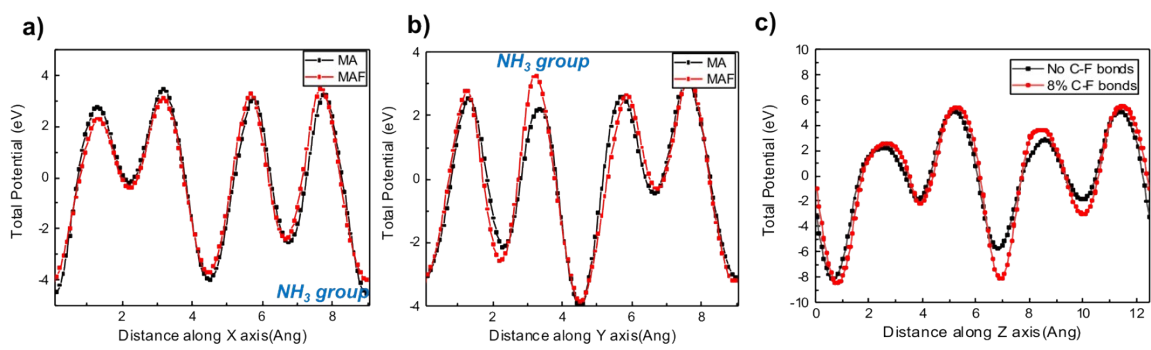

Figure S4. Total electrostatic potential V_I moving along the a) X and b) Y c) Z direction would have to cross within the 8% fluorinated MAPI tetragonal unit cell.
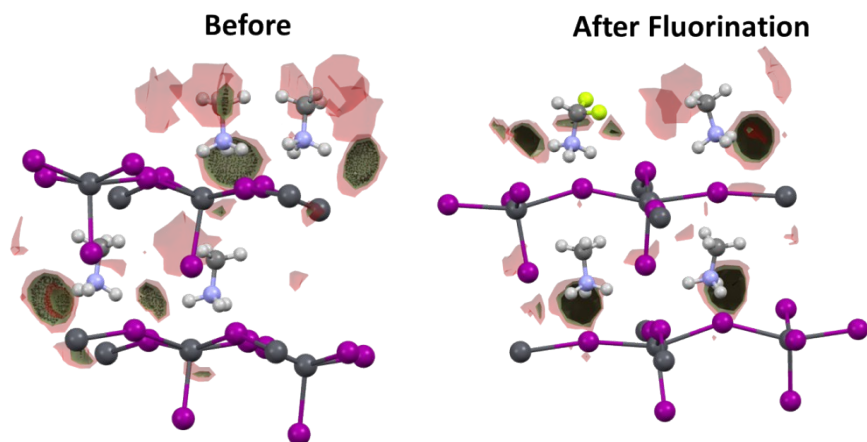
Before   **After Fluorination**

Figure S5. Water Interaction map of $CH_3NH_3PbI_3$ perovskite with oxygen-water before and after fluorination, demonstrating a noticeable increase in hydrophobicity. Contour gradients move form light to dark by moving from isovalues at 2.0, 4.0, 0.6.

References

[1] J. Contreras-Garcia, W. Yang, E. R. Johnson, J. Phys. Chem. A 2011, 115, 12983 –12990

[2] A. Otero-de-la-Roza, E. R. Johnson, J. Contreras-Garcıa, Phys. Chem. Chem. Phys. 2012, 14, 12165 –12172

[3] J. Contreras-Garcia, E. R. Johnson, S. Keinan, R. Chaudret, J.-P. Piquemal, D. N. Beratan, W. Yang, J. Chem. Theory Comput. 2011, 7, 625– 632.

TOC GRAPHICS
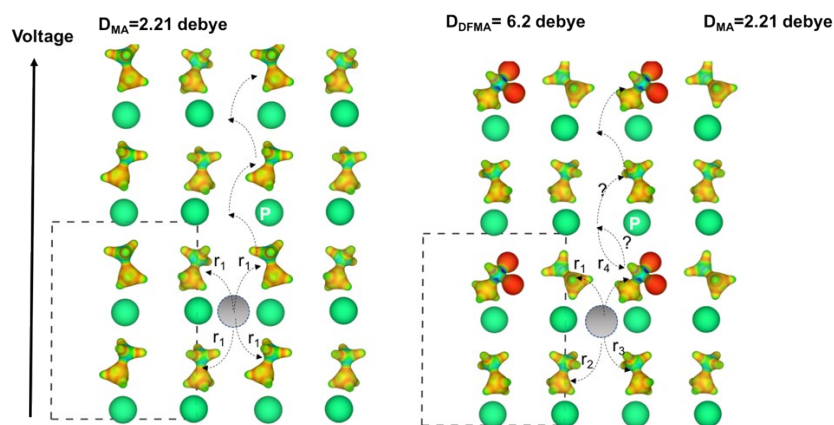
Electronic charge density in MAPI and MAPI with 8% DFMA, color maps correspond to the electrostatic potential, gray circle represent a moving ion such as iodine vacancies at different diffusion rates.